Author Manuscript

Author Manuscript

Author Manuscript

Author Manuscript

HHS Public Access

Author manuscript

J Control Release. Author manuscript; available in PMC 2017 December 10.

Published in final edited form as:

J Control Release. 2016 December 10; 243: 225–231. doi:10.1016/j.jconrel.2016.10.009.

Macroporous Acrylamide Phantoms Improve Prediction of *In Vivo* Performance of *In Situ* Forming Implants

Christopher Hernandez[1], **Natalia Gawlik**[1], **Monika Goss**[1], **Haoyan Zhou**[1], **Selva Jeganathan**[1], **Danielle Gilbert**[1], and **Agata A. Exner**[1,2]

[1]Department of Biomedical Engineering, Case Western Reserve University, 11100 Euclid Ave, Cleveland, OH, 44106 USA

[2]Department of Radiology Case Western Reserve University, 11100 Euclid Ave, Cleveland, OH, 44106 USA

Abstract

In situ forming implants (ISFIs) have shown promise as a sustained, local drug delivery system for therapeutics in a variety of applications. However, development of ISFIs has been hindered by poor correlation between *in vitro* study results and *in vivo* performance. In contrast to oral dosage forms, there is currently no clear consensus on a standard for *in vitro* drug dissolution studies for parenteral formulations. Recent studies have suggested that the disparity between *in vivo* and *in vitro* behavior of phase-inverting ISFIs may be, in part, due to differences in injection site stiffness. Accordingly, this study aimed to create acrylamide-based hydrogel phantoms of various porosities and stiffness, which we hypothesized would better predict *in vivo* performance. Implant microstructure and shape were found to be dependent on the stiffness of the phantoms, while drug release was found to be dependent on both phantom porosity and stiffness. Specifically, SEM analysis revealed that implant porosity and interconnectivity decreased with increasing phantom stiffness and better mimicked the microstructure seen *in vivo*. Burst release of drug increased from 31% to 43% when in standard acrylamide phantoms vs macroporous phantoms (10 kPa), improving the correlation to the burst release seen *in vivo*. Implants in 30 kPa macroporous phantoms had the best correlation with *in vivo* burst release, significantly improving ($p < 0.05$) the burst release relative to *in vivo* from 64%, using a standard PBS dissolution method, to 92%. These findings confirm that implant behavior is affected by injection site stiffness. Importantly, with appropriate optimization and validation, hydrogel phantoms such as the one investigated here could be used to improve the *in vitro-in vivo* correlation of *in situ* forming implant formulations and potentially augment their advancement to clinical use.

Graphical Abstract

To whom correspondence should be addressed: Agata A. Exner, PhD, Department of Radiology, Case Western Reserve University, 11100 Euclid Ave, Cleveland, OH, 44106-5056, 216-844-3544, agata.exner@case.edu.

Publisher's Disclaimer: This is a PDF file of an unedited manuscript that has been accepted for publication. As a service to our customers we are providing this early version of the manuscript. The manuscript will undergo copyediting, typesetting, and review of the resulting proof before it is published in its final citable form. Please note that during the production process errors may be discovered which could affect the content, and all legal disclaimers that apply to the journal pertain.

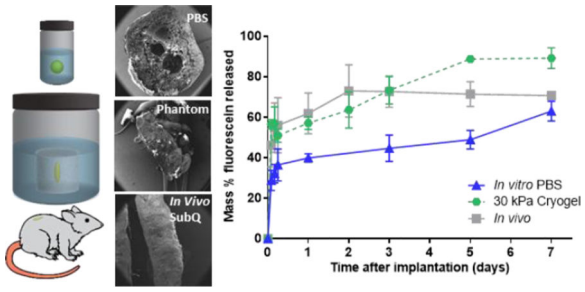

Keywords

in situ forming implant; In vitro-in vivo correlations (IVIVC); tissue mimicking phantoms; *in vitro* test; cryogel; drug delivery

1. Introduction

In situ forming implants (ISFI) for sustained delivery of therapeutics are an attractive alternative to oral and intravenous dosing as well as the conventional pre-formed drug eluting depots. They have been shown to be successful in delivering a diverse range of therapeutic agents, including local chemotherapeutics for intratumoral cancer treatment [1–5], doxycycline for the treatment of periodontal disease[6, 7], and sucrose acetate isobutyrate for the treatment of schizophrenia and bipolar disorder[8]. Phase-sensitive ISFIs, first patented by Dunn et al. in 1990, are made from a hydrolytically degradable and water insoluble polymer that is co-dissolved with a therapeutic agent in a water miscible organic solvent[9, 10]. Upon injection into tissue, the implants undergo a process of phase inversion, in which the organic solvent inside of an ISFI solution begins to diffuse out while simultaneously being replaced by water from the surrounding tissue, forming the precipitated water-insoluble polymer matrix[11, 12]. Unlike pre-formed drug-eluting implants that require surgical implantation, ISFI systems can be injected through a small needle directly into the site of action, improving patient comfort and compliance.

Despite these benefits, development and translation of these systems has been sluggish. This is in part due to poor *in vitro-in vivo* correlations (IVIVC) stemming from the influence of the injection site properties on the phase inversion and implant formation process. In many cases, the typical dissolution set-up does not take into account the mechanical properties of the milieu surrounding the implant[13]. Improving the IVIVC of phase inverting systems to accurately predict their bioperformance circumvents the high cost and ethical concerns associated with extended *in vivo* animal and human studies. The discrepancy between *in vitro/in vivo* behavior has been shown to be especially pronounced when delivering low molecular weight hydrophilic molecules[14, 15]. Recent work by Solorio et al. has shown that implants, made with PLGA and NMP, injected subcutaneously *in vivo* had increased burst release and rate of phase inversion when compared to those formed *in vitro* in a PBS bath[15]. As one may expect, these differences in implant behavior can be attributed to the ultimate implant shape, size, and microstructure. Implant size and shape are both influenced by the injection procedure and formulation[16], while implant microstructure has been

Author Manuscript Author Manuscript Author Manuscript Author Manuscript

Author Manuscript Author Manuscript Author Manuscript Author Manuscript

correlated to the rate of phase inversion[12, 17, 18]. ISFIs were originally intended to be injected into the subcutaneous or intramuscular space, which chemically speaking, can be considered to be a mixture of water, organic solvent, proteins and salts. This mixture is significantly different from solvents used in typical *in vitro* dissolution studies. Although only a few studies have been done to elucidate the effects of these bathside components[11, 12], none of them can account for the drastic differences in release profiles that lead to the poor IVIVC.

While the chemical composition of the injection site is important, the physical structure or tissue stiffness also plays a role in implant formation and drug release *in vivo*. Patel et al. investigated the effect of injection site stiffness on implant formation and release[14]. They found that when injected *in vivo*, implants were flatter with a less uniform shape as compared to the spherical implants that were formed when dropped in a PBS bath *in vitro*. More interestingly, they found that the deviation of *in vivo* burst release from *in vitro* correlated with implant polymer molecular weight. It was hypothesized that there is an increased osmolarity and solvent retention generated by more rapidly degrading low molecular weight PLGA. While this increased osmolarity leads to swelling of implants *in vitro*, the compressive forces of tissue inhibit implant expansion and therefore lead to a mechanically-induced convective release of solvent and drug efflux.

In order to further investigate the effect of injection site on performance of ISFIs, we have developed a series of *in vitro* hydrogel phantoms capable of constraining implant swelling to mimic the mechanical inhibition from *in vivo* tissue. These polyacrylamide phantoms provide a physical structure with high water content and tunable biologically-relevant mechanical properties. As ISFIs are moving towards more unconventional sites of injection, such as directly into tumors (which can be as stiff as 42 kPa [19]), we have investigated phantoms from ranging in elastic modulus from 1 to 30 kPa. In the current study, the effects of phantom stiffness and diffusion properties on drug release, implant microstructure, and swelling were evaluated.

2. Methods

2.1 Materials

Poly(DL-lactic-co-glycolic) (acid-capped PLGA, 50:50, MW 13.8 kDa) was obtained from Lactel, Durect Corp (AL), and used as received. N-methyl-2-pyrrolidinone (NMP) and sodium fluorescein were obtained from Sigma–Aldrich (St. Louis, Missouri). Acrylamide, bis-acrylamide, ammonium persulfate (APS), and N,N,N′,N′-tetramethylethylenediamine (TEMED) were obtained from Fisher Scientific, Waltham, MA.

2.2 ISFI solution preparation

ISFI polymer solutions were made from 13.8 kDa PLGA (inherent viscosity 0.19 dL/g) co-dissolved with a mock drug (fluorescein disodium salt) in NMP with a 60:39:1 mass ratio of solvent:polymer:drug. The components of the polymer solution were added together and allowed to dissolve overnight inside an incubator shaker at 37°C. Polymer solutions were used within 24 h of mixing.

Author Manuscript Author Manuscript Author Manuscript Author Manuscript

2.3 In vitro PBS release

For PBS studies, polymer solution (40 μl) was injected into 10 ml of PBS and placed inside an incubator shaker at 37° C and 80 rpm. The PBS solution was refreshed every 24 hours. At predetermined time points (t=2, 4, 6 h and 1, 2, 3, 5, 7 days), implants were harvested, weighed and degraded in 2M sodium hydroxide. Cumulative release of drug was determined by measuring the residual drug left in each implant at the time of harvest. Once degraded, the residual drug was determined by comparison to a standard curve using a plate reader at an excitation wavelength of 485 nm and an emission wavelength of 525 nm (Tecan Ltd, Infinite 200 series). The release at each time point was averaged from 3 implants.

2.4 In vivo release

All animal studies were performed following protocols approved by the Case Western Reserve University Institutional Animal Care and Use Committee. Briefly, 6–8 week old Sprague-Dawely rats (Charles River Laboratories Inc. Wilmington, MA) were anesthetized using 1% isoflurane with an oxygen flow rate of 1l/min. ISFI solution (120 μl) was injected under the ventral skin flap in four locations using a 21-gauge hypodermic needle. At predetermined time points (t=2, 4, 6 h and 1, 2, 3, 5, 7 days), implants were dissected out after euthanasia. Dissected implants were degraded and the residual drug left in each implant was determined as described earlier.

2.5 Phantom preparation and characterization

Phantoms of varying moduli and porosity were prepared as follows. Microporous polyacrylamide phantoms of varying moduli were made by varying the mass ratio of acrylamide in PBS. A 40% acrylamide solution was used to make phantom solutions ranging between 6.45 and 26.54 wt.% (Table1). Acrylamide solutions were then cross-linked by free radical polymerization with TEMED and APS inside 24 well plates at room temperature. Macroporous phantoms where made by a cryogelation technique that involves crosslinking under freezing conditions[20, 21].These solutions were cooled to 0° C in an ice water bath where TEMED and APS were added to initiate polymerization. The solution was then quickly poured into a 24 well plate and placed in a −20°C freezer for 24 h. After the incubation period, implants were allowed to thaw and swell in PBS for 24 h. All phantoms were cross-linked with 0.095 wt.% bisacrylamide.

Young’s modulus of acrylamide samples was determined by standard unconfined compressive mechanical testing using a rheometer (Rheometrics RSAII, NJ or Test Resources 800LE3-2, MN). Phantoms were polymerized inside 24 well plates, resulting in gels that were 15 mm in diameter and 20 mm in thickness. A strain rate of 0.01/s was used and the time for each compression test was optimized in order to achieve at least 30% strain. Young’s modulus was calculated using the linear range of the stress/strain curve. Microporous phantoms were tested at a predetermined time point spanning 14 days and stored in a solution of PBS (pH 7.4) inside an incubator shaker at 37° C in between testing. Macroporous phantoms swelled to the maximum level almost immediately, and therefore were only measured once.

Author Manuscript Author Manuscript Author Manuscript Author Manuscript

For swelling/ water uptake studies, microporous phantoms were again polymerized inside 24 well plates and weighed for their initial mass. Phantoms were then stored in a solution of PBS (pH 7.4) inside an incubator shaker at 37° C for 14 days. At pre-determined time points, samples were taken out of the PBS solution and weighed. Water uptake was calculated by dividing the final weight at each time point over the original weight of each phantom.

2.6 In vitro phantom drug release

For phantom release studies, acrylamide solutions were cross-linked inside 24 well plates. Macroporous and microporous phantoms were hydrated in PBS at 37° C degrees for one and five days, respectively. Once at steady state, 40 μl of ISFI solution were syringe injected into the center of each phantom. Phantoms were then placed in 100 ml of PBS inside in an incubator shaker at 37° C and 80 rpm. PBS was replenished daily. At predetermined time points (t= 2, 4, 6 h, and 1, 2, 3, 5,7 days), implants were harvested from phantoms, weighed, and degraded in 2M sodium hydroxide. Implants were degraded and the residual drug left in each implant was determined as described earlier. Fluorescent images of implants in phantoms were taken using the Maestro Imaging System. A blue excitation filter (435–480 nm) and a green emission filter (490 nm longpass filter) were used with a 10 ms exposure time.

2.7 Scanning electron microscopy

Implant microstructure was evaluated as previously described[15]. Briefly, harvested implants were freeze fractured and lyophilized for 2 days. Dry implants or phantoms were then sputter coated with 5 nm of palladium and imaged using a Quanta 200 3D ESEM (Hillsboro, OR) with an acceleration voltage of 3.5 kV and a hole size of 10 nm.

2.8 Statistical analysis

Statistical analysis was performed in GraphPad Prism using a two-tailed Student's *t*-Test ($p < 0.05$), assuming unequal variances between the two data sets. All data were reported as mean ± standard deviation and each data set contained a minimum of $n = 3$.

3. Results

3.1 In vitro and in vivo fluorescein release and water uptake

Fluorescein release kinetics from implants, formed either in a bath of PBS or in the subcutaneous space, demonstrated 2 phases; burst phase (24 h), and a diffusion phase (>24 h) (Fig 2a). Implants formed in the subcutaneous space had a significantly higher burst release than those formed in PBS (61.9 ± 10.0% vs 39.9 ± 2.1%, p< 0.05). The overall release at the end of the 7-day study was 70.7±1.9% and 63.0 ± 4.9% for implants formed *in vivo* and *in vitro*, respectively. Following the burst phase, release of fluorescein from implants formed *in vivo* was significantly reduced. Implants formed *in vitro* however, had a fluorescein release rate of 3.7% per day. Implants formed *in vitro* had a rapid uptake of fluid that continued until 5 days, reaching a maximum mass that was 3.8 fold higher than original mass (Fig. 2b). Implants formed *in vivo* reached a maximum mass at 24 h (2.3 fold),

Author Manuscript Author Manuscript Author Manuscript Author Manuscript

followed by a loss of mass until 3 days. Fluid uptake was significantly higher for implants formed *in vitro* as compared to those formed *in vivo* for all time points.

3.2 Mechanical properties of hydrogels

Polyacrylamide phantoms of different elastic moduli were fabricated by varying the ratio of acrylamide to PBS in the gel solution and tested under a standard unconfined compression test. The elastic modulus of the standard polyacrylamide gels was measured as-prepared, as well as after 5 and 14 days of swelling in PBS (Fig 1a). All samples had the highest elastic modulus immediately after polymerization, and equilibrated after 5 days. The elastic modulus of phantoms with an acrylamide wt.% of 6.45, 15.17 and 26.54% were 0.94±0.05, 10.39±0.50 and 18.19±0.44 kPa (for simplicity referred to as 1, 10, and 20 kPa phantoms), respectively after 5 days and did not have any statistically significant decreases after 14 days. Phantoms were weighed every other day to monitor their swelling/water-uptake over a 14-day period (Fig 1b). Microporous phantom swelling correlated well with increasing acrylamide wt.% and also equilibrated after 5 days in PBS. Macroporous phantom swelling plateaued within the first 24 hours at 240±30%, and 192±11% of their original mass for phantoms with an acrylamide wt.% of 15.17 and 34.12% (data not shown). The elastic modulus of macroporous phantoms was measured after 24 hours of swelling. The elastic modulus of macroporous phantoms with an acrylamide wt.% of 15.17, 26.54, and 34.12% was 8.68±2.24, 22.8±04.88 and 31.95±6.46 kPa (for simplicity, referred to as 10 kPa, 20 kPa and 30 kPa cryogel), respectively.

3.3 Drug release in standard phantoms

Implants injected into acrylamide microporous phantoms demonstrated three distinct phases of release; burst phase (<24 h), a plateau phase (24 to 72 h), and a diffusion phase (>72 h) (Fig. 3a). No statistical differences in the burst release of implants formed in phantoms were found. The overall release at the end of the study was 79.1±2.3, 86.2±4.8 and 98.8±0.3 for implants in 1, 10, and 20 kPa phantoms, respectively. The normalized peak mass of implants decreased with increasing phantom stiffness demonstrating the effect of injection site stiffness on implant swelling.

3.4 Drug release in macroporous phantoms

Implants formed in macroporous phantoms had an increased fluorescein release rate compared to those made in the microporous phantoms and lacked the plateau phase of the release profile (Fig. 4b). The increased release rate can be attributed to the increased diffusion of fluorescein through the large pores inside the phantoms made by cryogelation, as seen under SEM (Fig. 4a). This is also evident in the fluorescent images of the phantoms at 4 and 24 h after injection, in which increased penetration and distribution of fluorescein can be seen in the macroporous phantoms when compared to the microporous phantom (Fig. 4c). Average drug release was higher at all time points for implants in the 30 kPa cyrogel phantom compared to those in the 10 kPa cryogel phantoms (Fig. 4d). Implants in 20 kPa cyrogel phantoms had a slightly higher burst release than those in 10 kPa cryogel phantoms but was not statistically different than those in 30 kPa cryogel phantoms. When comparing the deviation of fluorescein release between *in vivo* to *in vitro*, the implants formed in the

Author Manuscript Author Manuscript Author Manuscript Author Manuscript

cryogels had a lower deviation than those formed in PBS for all time points up to 5 days (Fig. 5b).

3.5 Implant shape and microstructure

Implants formed in a PBS bath or in the subcutaneous space were found to have distinct microstructure (Fig 6). After 7 days, implants formed in a PBS bath were spherical, with a very porous and highly interconnected central domain. Implants formed *in vivo* had a smaller surface area, and lacked the porosity and interconnectivity seen in implants formed in a PBS bath. Implants formed in microporous phantoms exhibited microstructure in between that seen in PBS and *in vivo*. Porosity and interconnectivity of the center domain decreased with increasing phantom stiffness. Implant shape was also dependent on the injection site. When formed in PBS, implants were uniform and spherical throughout the entire study. Implants formed in the soft 1 kPa phantoms showed only marginal flattening while the stiff 10 and 20 kPa phantoms produced implants that were flat disk-shaped by the end of the 7-day study. Implants formed *in vivo* were also flat disk shaped at the end of the study.

4. Discussion

Predictive *in vitro* models are vital to reducing the cost and time associated with the progression to the clinical use of drug delivery systems. This has been especially true in the translation of phase-sensitive *in situ* forming implants (ISFIs), where their drug release can range from days to several months, leading to the high cost and ethical concerns associated with extended *in vivo* animal and human studies during formulation development. The current United States Pharmacopeia (USP) apparatus for *in vitro* release testing has been designed for oral and transdermal products and thus may not have great relevance for local ISFI use[13]. Unlike with oral formulations, there is no regulatory standard for parenteral drug delivery systems, resulting in an assortment of protocols for drug dissolution studies being reported in literature. While data suggest that implant behavior is sensitive to changes in injection environment, typical dissolution studies lack many of the physical and chemical properties of tissue, leading to poor IVIVC. The purpose of this study was to determine if a hydrogel phantom could mimic the injection environment forces exerted on an implant when injected *in vivo and* better predict *in vivo* performance.

As previously observed[14, 15], in the current study there were significant differences between implants formed *in vitro* in PBS and *in vivo*. Analysis under SEM revealed that implants formed *in vitro* in a PBS bath had a highly interconnected porous microstructure at the end of the 7-day study. Implants formed in the subcutaneous space however, had a dense polymer network with little interconnectivity at the end of study. Solorio et al. similarly observed this trend where the microstructure of implants formed *in vivo* initially resembled the highly porous and interconnected microstructure of those formed *in vitro*[15]. Over time however, only the implants formed *in vivo* showed a gradual loss of porosity. It was hypothesized that this change in porosity overtime leads to a loss of implant diffusivity, ultimately hampering drug release during the diffusion phase of implants formed *in vivo*. Implants formed *in vivo* also had a significantly higher burst release than implants formed *in*

Author Manuscript Author Manuscript Author Manuscript Author Manuscript

vitro. This disparity in burst release has been hypothesized to be a result of the compressive forces of tissue inhibiting implant expansion and therefore leading to a mechanically induced convective release of solvent and drug efflux.

In order to further investigate the effect of injection site stiffness on implant behavior, we developed polyacrylamide phantoms with different elastic moduli, capable of inhibiting implant swelling. The elastic moduli of these polyacrylamide phantoms were easily tuned by varying the mass ratio of acrylamide to PBS. For this study we formulated phantoms with three different moduli (1, 10 and 20 kPa), which covers the wide range of human soft tissue. These non-degradable phantoms, once water-equilibrated, had constant mechanical properties for over two weeks. When implants were formed in phantoms, analysis under SEM revealed that implant porosity was highly dependent on phantom stiffness. Implants formed in the soft 1 kPa phantoms had a microstructure similar to those formed in PBS with a highly porous and interconnected microstructure. Implants formed in the stiffer 10 or 20 kPa phantoms lacked this porosity and more closely resembled the implants that were formed *in vivo*. Implant shape was also dependent on the stiffness of the phantom. While all implants were initially spherical upon injection, the external pressure of the phantom on the implants resulted in their compression and flattening. Implants formed in the soft 1 kPa phantoms showed only marginal flattening while the stiff 10 and 20 kPa phantoms produced implants that were flat disk-shaped by the end of the 7-day study.

Although unexpected, phantom stiffness did not have an effect on the burst release from implants. Between 1 and 2 days after injection, no significant release of fluorescein from implants occurred in phantoms. We speculated that this could be attributed to the low permeability coefficient of highly cross-linked gels, which creates a higher accumulation of fluorescein outside of the implant and reduces the rate of fluorescein release. In order to circumvent this issue, macroporous phantoms were created by polymerizing polyacrylamide solutions under freezing conditions. Freezing the acrylamide solution prior to polymerization leads to polycrystals of frozen solvent surrounded by an unfrozen liquid microphase (ULMP) of highly concentrated monomers[20, 21]. These polycrystals serve as pore formers while the ULMP polymerizes around them.

At the conclusion of the study, SEM analysis of implants injected into 10 kPa macroporous hydrogels revealed the same dense polymer microstructure as seen in 10 kPa standard acrylamide phantoms (Fig. 5). However, fluorescent images of the phantoms at 30 min, 4 and 24 h after injection revealed that macroporous hydrogels had a greater distribution of fluorescein throughout the phantom, which was likely a result of higher permeability. The increased permeability resulted in fluorescein release kinetics from implants which did not display the plateau phase seen in the microporous phantoms. Implants formed in the stiffer 30 kPa macroporous phantoms had a significantly higher burst release (57.3±3.2 vs 43.25±4.2 vs 39.86±2.1%) when compared to implants formed in the softer 10 kPa phantoms and PBS. Implants in 20 kPa phantoms were shown to have a slightly increased burst release from 10 kPa, but the burst was not statistically different from 30kPa phantoms. We suspect that differences drug release from implants in this system are only sensitive to large increases in injection site stiffness and that the large pore size leads to equivalent permeability in these phantoms. As mentioned earlier, many factors can contribute to

Author Manuscript Author Manuscript Author Manuscript Author Manuscript

difference in burst release between implants formed in a PBS bath and those *in vivo*. However, evidence suggests that the disparity in burst release is largely due to the implants' inability to swell freely *in vivo*[14]. Our data supports this hypothesis, as implants formed in stiffer gels have been shown to be more compressed and have a higher burst release than those in PBS. The burst release from implants in the 30 kPa macroporous phantoms was found to better represent the burst release *in vivo* (57.2±3.2 vs 61.9±10.4%) than implants formed in PBS. The release rate from these implants in the 10 kPa phantom after 24 h was 2 fold higher (8.0 vs 3.7% per day) when compared to those formed in PBS. This increased release rate is likely attributed to the increased surface area to volume ratio of the flat disk-shaped implants.

This study has several limitations. In order to reduce matrix/drug interactions and limit toxicity, fluorescein disodium salt was used as a mock drug. It has been shown that fluorescein and the chemotherapeutic agent doxorubicin have similar release profiles from phase sensitive ISFIs, thus we expect that the result seen here would be applicable to this commonly utilized anticancer agent [18]. Additionally, this study was limited to the use of one polymer type with a specific molecular weight. Future studies should investigate higher molecular weight PLGA as well as other polymers used in phase sensitive ISFIs. Likewise, while it is likely that the effects of the injection site will have a bearing on most other injectable formulations, it is difficult to predict this behavior for systems that are driven by processes other than phase inversion (e.g. temperature or pH). Additional studies are required to demonstrate this effect is more broadly applicable.

5. Conclusions

Phase sensitive ISFIs implanted in tissue-mimicking phantoms were shown to better predict *in vivo* behavior than those done in a standard PBS dissolution study. While other studies have explored the effect of injection site stiffness on implant behavior *in vivo*, this is the first time an *in vitro* test was developed to mimic mechanical properties of tissues on implant behavior. Our findings suggest that the stiffness of the phantom has a direct effect on implant microstructure and mock drug release. Therefore, adaptation of these tissue-mimicking phantoms as the standard method for dissolution studies can improve the *in vitro-in vivo* correlations of ISFI and reduce the cost and time associated with clinical approval. 6.

Acknowledgments

This work was supported by the National Institute of Biomedical Imaging and Bioengineering and National Cancer Institute of the National Institutes of Health under award numbers R01EB016960, T32-EB007509, and F31CA200373. Views and opinions of, and endorsements by the author(s) do not reflect those of the National Institutes of Health.

References

1. Lee JY, Kim KS, Kang YM, Kim ES, Hwang SJ, Lee HB, Min BH, Kim JH, Kim MS. In vivo efficacy of paclitaxel-loaded injectable in situ-forming gel against subcutaneous tumor growth. Int J Pharmaceut. 2010; 392:51–56.
2. Gao W, Zheng YY, Wang RH, Chen HR, Cai XJ, Lu GM, Chu L, Xu CY, Zhang N, Wang ZG, Ran HT, Li P, Yang CJ, Mei ZC, Song JL. A smart, phase transitional and injectable DOX/PLGA-Fe

Author Manuscript Author Manuscript Author Manuscript Author Manuscript

implant for magnetic-hyperthermia-induced synergistic tumor eradication. Acta Biomater. 2016; 29:298–306. [PubMed: 26432438]

3. Li J, Krupka T, Yao JP, Wang RH, Jiang L, Zhou Y, Zuo GQ, Wang ZB, Dai LL, Ren JL, Zheng YY, Wang D. Liquid-Solid Phase-Inversion PLGA Implant for the Treatment of Residual Tumor Tissue after HIFU Ablation. Plos One. 2015; 10
4. Vejjasilpa K, Nasongkla N, Manaspon C, Larbcharoensub N, Boongird A, Hongeng S, Israsena N. Antitumor efficacy and intratumoral distribution of SN-38 from polymeric depots in brain tumor model. Exp Biol Med. 2015; 240:1640–1647.
5. Manaspon C, Hongeng S, Boongird A, Nasongkla N. Preparation and in vitro characterization of SN-38-loaded, self-forming polymeric depots as an injectable drug delivery system. J Pharm Sci-Us. 2012; 101:3708–3717.
6. Stoller NH, Johnson LR, Trapnell S, Harrold CQ, Garrett S. The pharmacokinetic profile of a biodegradable controlled-release delivery system containing doxycycline compared to systemically delivered doxycycline in gingival crevicular fluid, saliva, and serum. J Periodontol. 1998; 69:1085–1091. [PubMed: 9802705]
7. Do MP, Neut C, Metz H, Delcourt E, Mader K, Siepmann J, Siepmann F. In-situ forming composite implants for periodontitis treatment: How the formulation determines system performance. Int J Pharmaceut. 2015; 486:38–51.
8. Lu YX, Yu YL, Tang X. Sucrose acetate isobutyrate as an in situ forming system for sustained risperidone release. J Pharm Sci-Us. 2007; 96:3252–3262.
9. Dunn RL, Tipton AJ. Polymeric compositions useful as controlled release implants. Google Patents. 1997
10. Dunn RL, English JP, Cowsar DR, Vanderbilt DP. Biodegradable in-situ forming implants and methods of producing the same. Google Patents. 1990
11. Brodbeck KJ, DesNoyer JR, McHugh AJ. Phase inversion dynamics of PLGA solutions related to drug delivery. Part II. The role of solution thermodynamics and bath-side mass transfer. J Control Release. 1999; 62:333–344. [PubMed: 10528071]
12. Graham PD, Brodbeck KJ, McHugh AJ. Phase inversion dynamics of PLGA solutions related to drug delivery. J Control Release. 1999; 58:233–245. [PubMed: 10053196]
13. Burgess DJ, Hussain AS, Ingallinera TS, Chen ML. Assuring quality and performance of sustained and controlled release parenterals: AAPS workshop report, co-sponsored by FDA and USP. Pharm Res. 2002; 19:1761–1768. [PubMed: 12458685]
14. Patel RB, Solorio L, Wu H, Krupka T, Exner AA. Effect of injection site on in situ implant formation and drug release in vivo. J Control Release. 2010; 147:350–358. [PubMed: 20728486]
15. Solorio L, Exner AA. Effect of the Subcutaneous Environment on Phase-Sensitive In Situ-Forming Implant Drug Release, Degradation, and Microstructure. J Pharm Sci. 2015; 104:4322–4328. [PubMed: 26506522]
16. Kempe S, Mader K. In situ forming implants - an attractive formulation principle for parenteral depot formulations. J Control Release. 2012; 161:668–679. [PubMed: 22543012]
17. Solorio L, Sundarapandiyan D, Olear A, Exner AA. The Effect of Additives on the Behavior of Phase Sensitive In Situ Forming Implants. J Pharm Sci-Us. 2015; 104:3471–3480.
18. Solorio L, Olear AM, Zhou HY, Beiswenger AC, Exner AA. Effect of cargo properties on in situ forming implant behavior determined by noninvasive ultrasound imaging. Drug Deliv Transl Re. 2012; 2:45–55.
19. Samani A, Zubovits J, Plewes D. Elastic moduli of normal and pathological human breast tissues: an inversion-technique-based investigation of 169 samples. Phys Med Biol. 2007; 52:1565–1576. [PubMed: 17327649]
20. Carvalho BMA, Da Silva SL, Da Silva LHM, Minim VPR, Da Silva MCH, Carvalho LM, Minim LA. Cryogel Poly(acrylamide): Synthesis, Structure and Applications. Sep Purif Rev. 2014; 43:241–262.
21. Plieva F, Xiao HT, Galaev IY, Bergenstahl B, Mattiasson B. Macroporous elastic polyacrylamide gels prepared at subzero temperatures: control of porous structure. J Mater Chem. 2006; 16:4065–4073.

Author Manuscript Author Manuscript Author Manuscript Author Manuscript

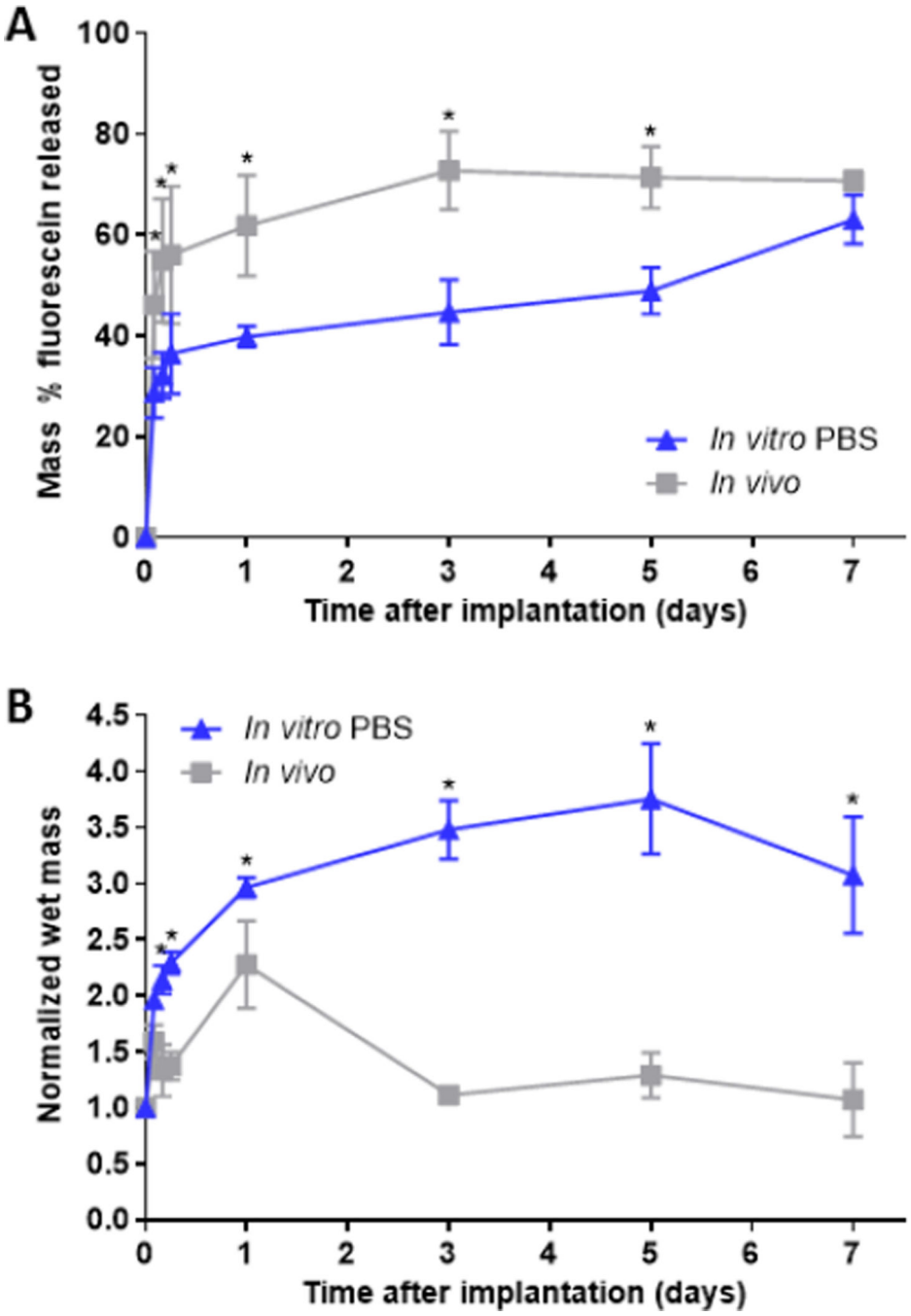

Figure 1.

(A) Cumulative mass release of fluorescein and (B) Normalized wet mass of implants over the course of 7 days. Implants were formed in PBS and subcutaneously under the ventral skin flap of Sprague-Dawley rats. * indicates $p < 0.05$.

Author Manuscript Author Manuscript Author Manuscript Author Manuscript

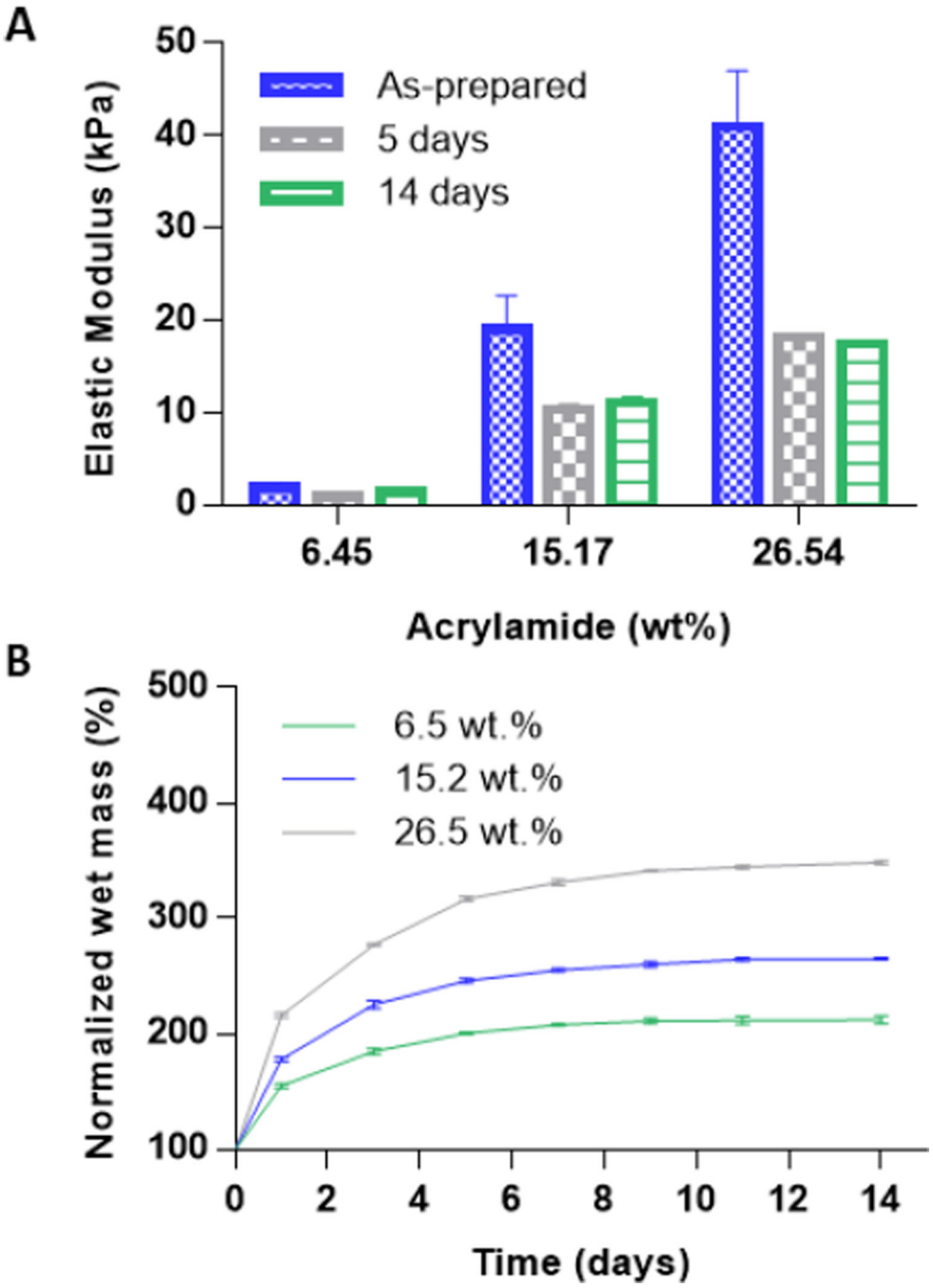

Figure 2.
Change in mass of standard polyacrylamide phantoms during equilibrium swelling in PBS.

Author Manuscript Author Manuscript Author Manuscript Author Manuscript

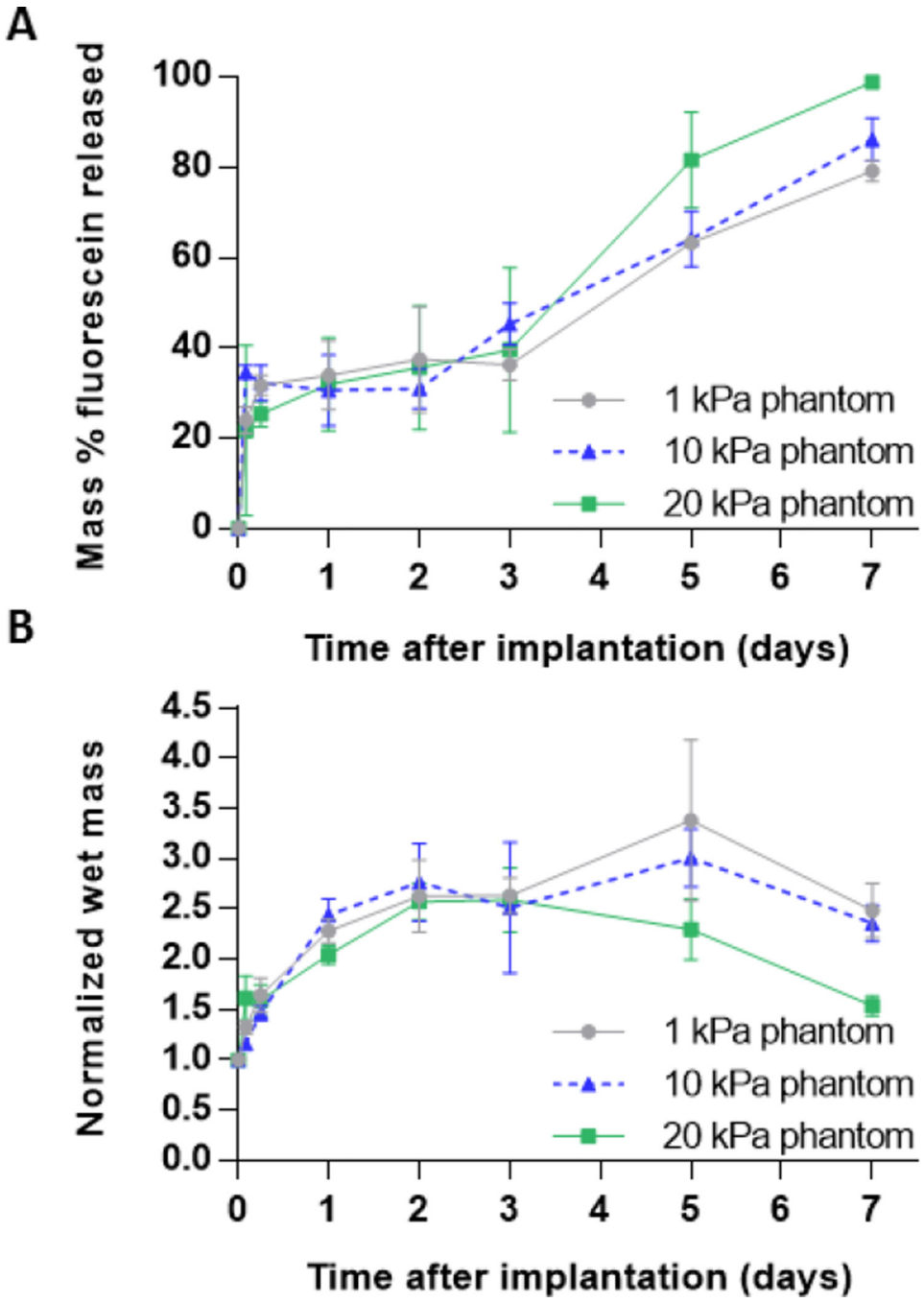

Figure 3.
(A) Cumulative mass release of fluorescein and (B) Normalized wet mass of implants over the course of 7 days for implants injected into standard acrylamide phantoms of varying elastic moduli.

Author Manuscript Author Manuscript Author Manuscript Author Manuscript

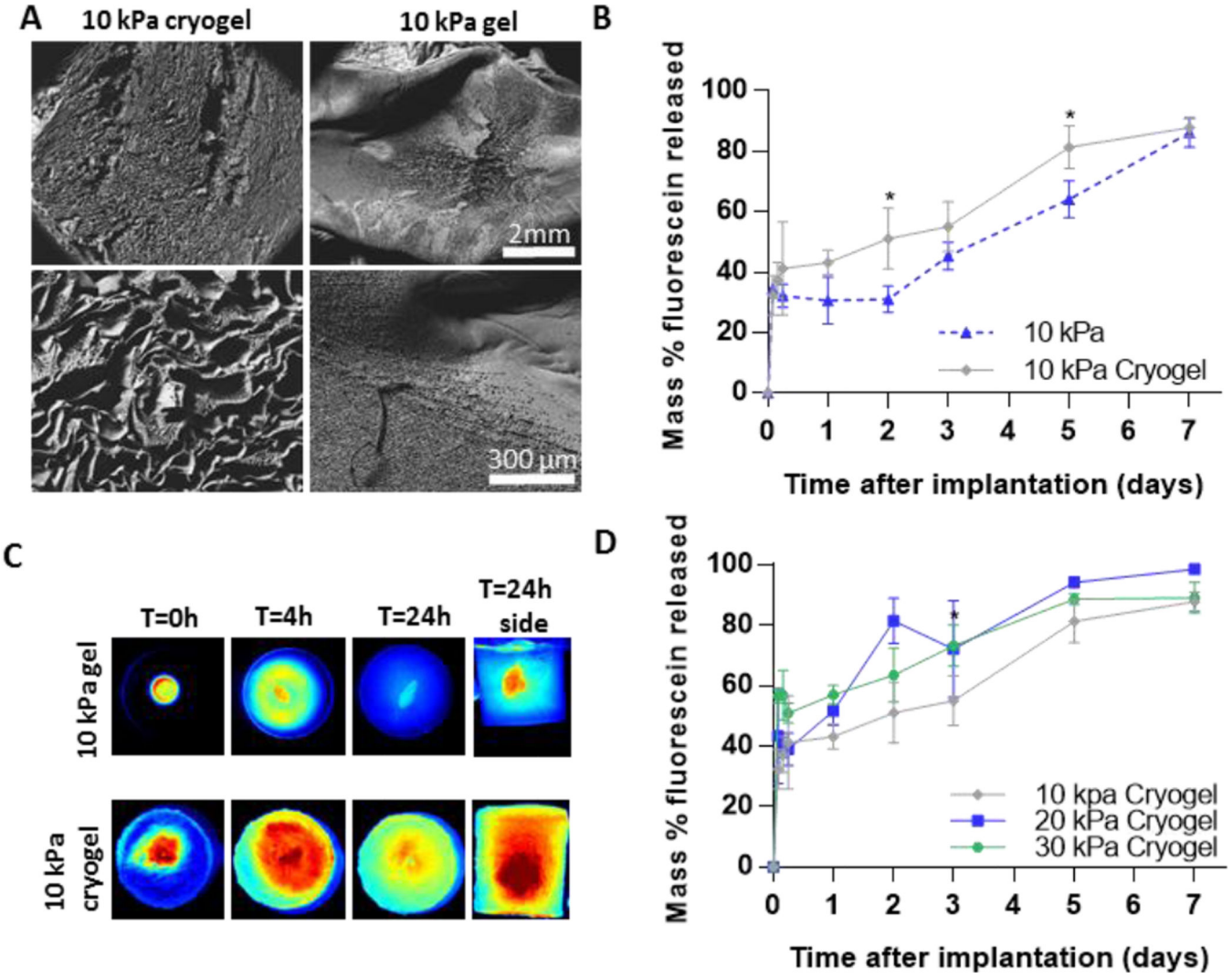

Figure 4.

(A) SEM image of standard and cryogel phantoms (B) Cumulative percent release of mock drug from standard and cryogel phantom (C) Fluorescent images of phantoms over 24 h. (D) Cumulative percent release of mock drug from cryogel phantoms. * indicates $p < 0.05$.

Author Manuscript Author Manuscript Author Manuscript Author Manuscript

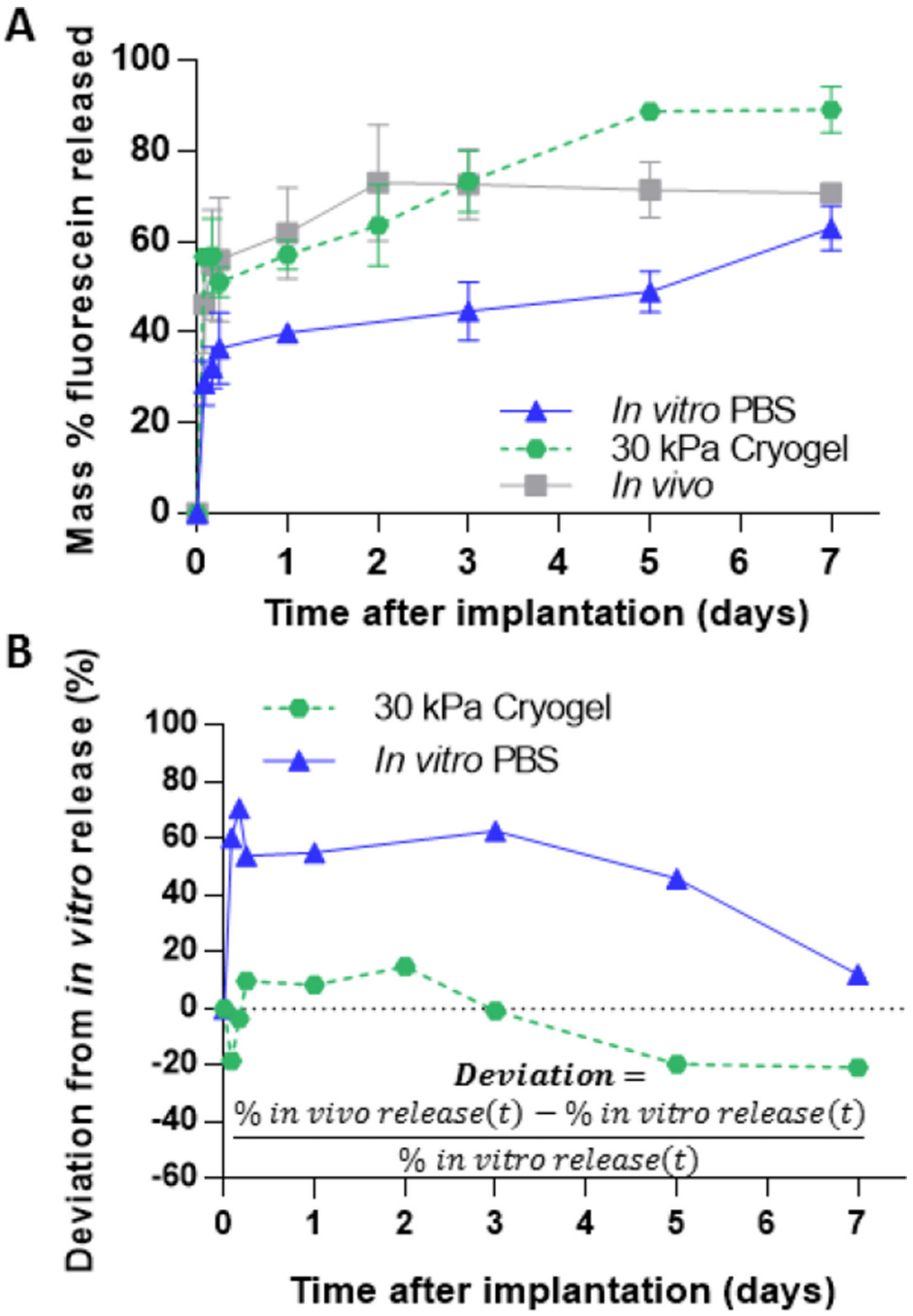

Figure 5.

(A) Cumulative mass of fluorescein released from three different environments (B) Deviation of *in vivo-in vitro* fluorescein release from implants formed in varying *in vitro* environments

Author Manuscript Author Manuscript Author Manuscript Author Manuscript

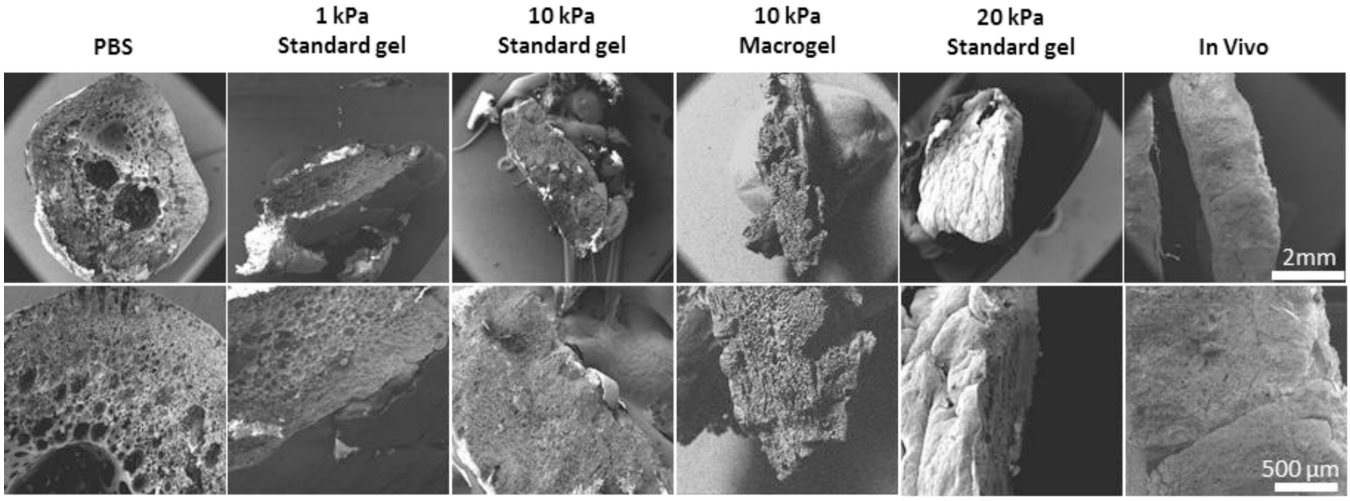

Figure 6.

Scanning electron microscopy images highlighting the difference in microstructure for implants formed in the subcutaneous space and *in vitro*.

Author Manuscript Author Manuscript Author Manuscript Author Manuscript

Table 1

Formulations for polyacrylamide phantoms

	Acrylamide	Bis-acrylamide	Solvent	APS	TEMED
Standard	(1.7, 6.4)	(0.5, 0.095)	7.8	0.5	50
	(4.0, 15.2)	(0.5, 0.095)	5.5	0.5	50
	(7.0, 26.5)	(0.5, 0.095)	2.5	0.5	50
Macrogels	(4.0, 15.2)	(0.5, 0.095)	5.5	0.16	20
	(7.0, 26.5)	(0.5, 0.095)	5.5	0.16	20
	(9.0, 34.12)	(0.5, 0.095)	0.5	0.16	20
	(ml, wt%)	**(ml, wt%)**	**(ml)**	**(ml)**	**(μl)**